

- ²⁴24, 942 (1970).
- ²²M. Cardona and F. H. Pollak, Phys. Rev. **142**, 530 (1966).
- ²³The deformation potential \mathcal{E}_2^* is equal to that used in Ref. 12 (Ξ_μ^*).
- ²⁴H. J. McSkimin, J. Appl. Phys. **24**, 988 (1953).
- ²⁵S. Zwerdling, K. J. Button, B. Lax, and L. M. Roth, Phys. Rev. Letters **4**, 173 (1960).
- ²⁶D. Brust and L. Liu, Solid State Commun. **4**, 193 (1966).
- ²⁷F. Cerdeira, J. S. de Witt, U. Rössler, and M. Cardona, Phys. Status Solidi **41**, 735 (1970).
- ²⁸J. C. Hensel and K. Suzuki, Bull. Am. Phys. Soc. **14**, 113 (1969).
- ²⁹I. Goroff and L. Kleinman, Phys. Rev. **132**, 1080 (1963).
- ³⁰P. J. Melz, Harvard University Technical Report No. HP-25, 1969 (unpublished).
- ³¹W. Paul and G. L. Pearson, Phys. Rev. **98**, 1755 (1955).
- ³²D. Warschauer and W. Paul, J. Phys. Chem. Solids **5**, 102 (1958).
- ³³M. Nathan and W. Paul, Phys. Rev. **128**, 38 (1962).
- ³⁴I. Balsley, J. Phys. Soc. Japan Suppl. **21**, 101 (1966).
- ³⁵G. S. Hobson and E. G. S. Paige, Proc. Phys. Soc. (London) **88**, 437 (1966).
- ³⁶E. Anastassakis, A. Pinczuk, E. Burstein, F. H. Pollak, and M. Cardona, Solid State Commun. **8**, 133 (1970).
- ³⁷E. O. Kane, in *Semiconductors and Semimetals*, edited by R. K. Willardson and A. C. Beer (Academic, New York, 1967), Vol. 1, p. 75.
- ³⁸J. O. Dimmock, Ref. 37, Vol. 3, p. 296.

Band-Tail Model for Optical Absorption and for the Mobility Edge in Amorphous Silicon

Frank Stern

IBM Watson Research Center, Yorktown Heights, New York 10598

(Received 18 November 1970)

The potential in amorphous Si is assumed to be the crystalline potential perturbed by a fluctuating potential with a root-mean-square amplitude V_{rms} and a correlation length L . The density of states for such a perturbing potential is taken from the work of Halperin and Lax. The optical absorption is calculated using effective-mass-approximation envelope wave functions whose degree of localization depends on energy. A good fit to optical-absorption data for amorphous Si films annealed at room temperature is obtained using $V_{\text{rms}} = 0.89$ eV and $L = 6$ Å, provided the wave-vector separation between the conduction- and valence-band edges is reduced from 9.5×10^4 to 6×10^7 cm⁻¹. The mobility edge is found from an extension to the model which gives an effective bandwidth W and a spacing parameter r_s , each as a function of energy. The mobility edge E_m lies approximately where $W(E_m) = \frac{2}{3} V_{\text{rms}}$. The mobility near the mobility edge is estimated from a diffusion model to be 5 cm²/V sec, and the density of states at the edge is 10^{21} cm⁻³ eV⁻¹.

I. INTRODUCTION

A substantial body of information has accumulated concerning the properties of amorphous semiconductors, particularly in the last two years.¹ Many models for describing the properties of these materials have evolved,^{2,3} and some features of these models are reflected in the work reported in this paper. We calculate the electrical and optical properties of amorphous Si from a model which assumes that the amorphous material is a strongly perturbed crystal. That is, we start with the energy gap, dielectric constant, and effective masses of the crystal, introduce a strong randomly varying perturbing potential of a particular form, and ask for the resulting density of states, wave functions, optical absorption, and dc conductivity.

In the course of the calculation we make many assumptions and approximations. Some of these are justified by qualitative reasoning, guided by knowledge of the behavior at high or low energies.

Others are made simply to permit numerical results to be obtained without excessive computation. We believe that the resulting model has the advantage of allowing the microscopic properties of the system to be exhibited quantitatively.

The model is applied to amorphous Si, whose optical and electrical properties have been investigated by many authors, and for which the relevant parameters of the crystal are well known. The method is applicable to other amorphous semiconductors, such as the chalcogenides and their alloys, provided band-structure parameters and dielectric constants are known.

II. DENSITY OF STATES

The first quantity we need to know is the density of states in each band. Throughout the calculation we adopt the sign convention that energies in the tail are negative and energies well into the band are positive, and use the nominal (i.e., unperturbed) band edge as the zero of energy for each

band. The periodic potential of the crystal is assumed to be perturbed by a fluctuating potential $V(\vec{r})$ whose correlations from point to point are characterized on the average by

$$\langle V(\vec{r}) V(\vec{r}') \rangle = V_{\text{rms}}^2 e^{-|\vec{r}-\vec{r}'|/L} \quad (1)$$

Halperin and Lax⁴ calculated the density of states for such a potential, and also displayed some properties of the wave functions. In their paper they considered specifically the fluctuating potentials that arise from randomly placed screened Coulomb centers. In that case L is the screening length and V_{rms} can be calculated from L and the ion concentrations.

We do not propose that the random potentials in amorphous semiconductors arise from Coulomb centers. However, we do postulate that the fluctuating potentials can be characterized by Eq. (1), and we take the correlation length L for amorphous semiconductors to be a measure of the distance over which short-range order is observed in the radial distribution function.⁵ For amorphous Si we use $L = 6 \text{ \AA}$. The magnitude V_{rms} of the fluctuations is left as an adjustable parameter. Potentials of the form (1) have been discussed in the present context by Bonch-Bruевич.⁶

The fluctuating potential (1) is assumed in this work to be the only perturbation of the periodic potential of the crystalline material. We ignore the additional effects that may arise from density changes^{7,8} or from states associated with internal surfaces or dangling bonds.⁹

If the quantities L and V_{rms} that characterize the fluctuating potential are known, then the theory of Halperin and Lax gives numerical results for the density of states in each band. One uncertainty in the application of their results is that they did not consider in detail the consequences of multivalley, nonparabolic, or degenerate band structures. Thus, it is not clear what value of effective mass to use in their expressions. The effective mass which we use in Eqs. (5.9) and (5.22) of Halperin and Lax is the conductivity or susceptibility mass m_s ,¹⁰ which does not count multiple valleys. It may not weight the individual mass components correctly.¹¹ A more realistic treatment of general band structures is likely to lead to more complicated results than those obtained by Halperin and Lax, so that we must make a reasonable choice for effective-mass values and must expect that the results will be only approximate.

The Halperin-Lax results are valid only in a limited energy range. They fail far in the tail because the model does not treat large values of the potential fluctuations correctly. The results are also invalid near or above the nominal band edge because Halperin and Lax omitted excited states and considered only the lowest state in any one

potential well formed by the fluctuating potential. Thus we need a way to interpolate between their results for the band tail and the high-energy region of the band where the unperturbed density of states is a good approximation.

One possible way to interpolate between the two results is to use an expansion in moments of the density of states, using the work of Kane.¹² At energies well above the nominal band edge, the original theory of Kane¹³ and others¹⁴ will apply, and at energies in the tail the Halperin-Lax results apply. In many cases the energy region in which neither approximation holds is quite large, and the moment expansion method may be difficult to use because many moments will be required. We have not tried to use it.

To obtain a smooth density of states for the entire energy range we used a Kane function [Eq. (48) of Ref. 13] characterized by a parameter η whose value is chosen so that the resulting density of states agrees with the Halperin-Lax values at one energy. The matching is done where $b(\nu) = 10\xi'$ in the Halperin-Lax notation, somewhat below the estimated upper limit of validity ($b \sim 6\xi'$) of their results. In the original Kane theory the parameter η is equal to $V_{\text{rms}}\sqrt{2}$. The matching results in smaller values of η , the exact value depending on the effective masses of the band and on the correlation length L .

III. WAVE FUNCTION

Having matched the Halperin-Lax density of states in the band tail to the unperturbed density of states at high energy by using a Kane function, we now need a way to estimate the wave function for each energy in this range. The wave functions obtained by Halperin and Lax are real, and correspond to states localized in individual potential wells associated with the fluctuating potential. At high energies in the band the effect of the potential fluctuations will be small and the states can be represented as plane waves. In the intermediate energy range we use an approximate wave function to interpolate between these two limiting forms.

The approximate wave function we use is the product of an effective-mass-approximation envelope wave function of a particular form and the wave function at the bottom of the band. We take the wave function for a state of energy E_i in band i to be

$$\psi_i(E_i; \vec{r}) \sim e^{i\vec{k}_i \cdot \vec{r}} e^{-\beta_i |\vec{r}-\vec{r}_{i0}|} e^{i\vec{k}_{i0} \cdot \vec{r}} u_i(\vec{r}), \quad (2)$$

where \vec{r}_{i0} is the point near which the wave function is localized, \vec{k}_{i0} is the wave vector associated with the edge of band i , and $u_i(\vec{r})$ is the corresponding periodic Bloch function. Normalizing factors are omitted here for simplicity. Equation (2) gives the approximate wave function near \vec{r}_{i0} ; the global

TABLE I. Summary of mobility-edge results for the valence and conduction bands of amorphous Si at 300 °K, calculated with a correlation length of 6 Å.

	$V_{\text{rms}} = 0.89 \text{ eV}$		$V_{\text{rms}} = 0.75 \text{ eV}$	
	Valence band	Conduction band	Valence band	Conduction band
Kane parameter $\eta(\text{eV})^a$	0.66	0.48	0.53	0.38
Mobility edge $E_m(\text{eV})^b$	-0.11	-0.20	-0.10	-0.17
Fermi energy $E_F(\text{eV})^b$	-0.65	-0.47	-0.66	-0.46
Mobility above $E_m(\text{cm}^2/\text{V sec})$	4.4	5.1	4.6	5.5
Density of states at $E_m(\text{cm}^{-3} \text{ eV}^{-1})$	1.2×10^{21}	9.4×10^{20}	1.0×10^{21}	7.7×10^{20}
Density of states at $E_F(\text{cm}^{-3} \text{ eV}^{-1})$	1.8×10^{20}	2.4×10^{20}	7.7×10^{19}	1.0×10^{20}
Carrier concentration $n, p(\text{cm}^{-3})$	3.7×10^{19}	3.7×10^{19}	1.2×10^{19}	1.2×10^{19}
Carriers above E_m $n_x, p_x(\text{cm}^{-3})$	2×10^{10}	7×10^{14}	1×10^{10}	2×10^{14}
Conductivity $(\Omega^{-1} \text{ cm}^{-1})$	2×10^{-3}	5×10^{-4}	8×10^{-3}	2×10^{-4}
Extrapolated conductivity $C(\Omega^{-1} \text{ cm}^{-1})^c$	210	190	180	170
x_s at E_m	0.9	0.8	0.9	0.8
E_m/η	-0.17	-0.42	-0.19	-0.45
$k(E_m)/\beta(E_m)$	1.75	1.62	1.65	1.50

^aSee Ref. 13.^bEnergies measured from nominal band edge; negative in the tail.^cAssumes an activation energy with a temperature coefficient $-2 \times 10^{-4} \text{ eV}/^\circ\text{K}$. See Eqs. (14) and (15).

behavior of the wave function throughout the sample is discussed in Sec. V.

Our prescription for calculating k_i and β_i is

$$\hbar^2 k_i^2 / 2m_{d,i} = E'_i, \quad (3a)$$

$$\hbar^2 \beta_i^2 / 2m_{s,i} = E_{\text{loc},i}, \quad (3b)$$

where $m_{d,i}$ and $m_{s,i}$ are the density-of-states and susceptibility (or conductivity) masses of band i , and E'_i is the energy below which there are as many states in the unperturbed band as there are states below E_i in the perturbed band. $E_{\text{loc},i}$ is the kinetic energy of localization for the state E_i , which we identify with the Halperin-Lax energy TE_Q , with T as given in their Table I. Since their results apply to only part of the energy range, we take the localization energy for all energies to be

$$E_{\text{loc},i} = h_i(E'_i - E_i), \quad (4)$$

where the constant h_i is obtained by matching the the Halperin-Lax results at the same energy at which the density of states is matched to the Kane function. The value of h_i depends on the correlation length L and on the effective masses, and is generally somewhat less than unity.

The energies E_i and E'_i are shown schematically in Fig. 1, and the values of E'_i and of $E'_i - E_i$ are shown as functions of E_i in Fig. 2. At high energies, $E' \sim E$ and the wave function (2) is bandlike; at low energies, $E' \sim 0$ and the wave function is

localized.

Why did we use the density-of-states mass for Eq. (3a) and the susceptibility mass for (3b)? The use of the density-of-states mass in (3a) is justified because that choice gives the correct limiting behavior at energies far up in the band, where E' is approximately equal to E . The use of the susceptibility mass in (3b) is not as well justified. The comments made in Sec. II in discussing the effective masses to be used in the Halperin-Lax equations also apply here.

The numerical values we use for amorphous Si with $V_{\text{rms}} = 0.89 \text{ eV}$ are

$$\begin{aligned} m_{d,c} &= 1.12m, & m_{d,v} &= 0.87m, \\ m_{s,c} &= 0.29m, & m_{s,v} &= 0.50m, \\ h_c &= 0.49, & h_v &= 0.38. \end{aligned} \quad (5)$$

The masses include an empirical allowance for nonparabolicity which is described elsewhere.¹⁵ The values are weak functions of V_{rms} and of temperature, but these variations do not have a major effect on our results. Note that the split-off valence band is not explicitly included in this calculation.

The effective-mass approximation, which underlies the approximate wave function (2), is valid for weak slowly varying perturbations, but is not likely to be well justified when the fluctuations are large in magnitude and have a short range, as we shall find to be the case for amorphous Si. However,

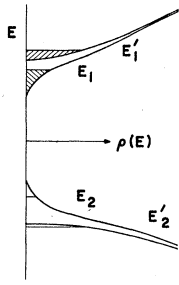


FIG. 1. Schematic density of states showing the energies E and E' in each band.

the effective-mass approximation probably applies better for Si than for semiconductors in which the energy gap is small (for example, InSb), or in which several bands lie close together in energy (for example, Ge), for which the wave function (2) would have to be replaced by a wave function which includes contributions from several bands.

The wave function (2) is not the solution of a Schrödinger equation; such solutions have not been obtained over the entire energy range for fluctuating potentials of the form (1). The usefulness of the model we propose depends on the degree to which the behavior of the actual system is adequately characterized by this approximate wave function. The accuracy of our results also depends on the accuracy of the density of states, because the parameter E' which enters in the determination of \tilde{k} and β is based on the density of states.

IV. OPTICAL ABSORPTION

The optical-absorption¹⁶ coefficient α is given by

$$\alpha(E) = G \int \rho_c(E_1) \rho_v(E_2) M_{av}^2(E_1, E_2) [f_2(E_2) - f_1(E_1)] dE_1 \quad (6a)$$

in the one-electron approximation, where ρ_c and ρ_v are the densities of states in the conduction and valence bands, respectively, f_1 and f_2 are the probabilities that the conduction- and valence-band states are occupied by electrons, and M_{av}^2 is the average squared matrix element for the transition between a state of energy E_1 in the conduction band and a state of energy E_2 in the valence band, averaged over polarization directions of the radiation and over electron spin orientations.^{17,18} The coefficient in (6a) is

$$G = 4\pi^2 e^2 \hbar / m^2 N E c, \quad (6b)$$

where e is the magnitude of the electron charge, m is the free-electron mass, N is the index of refraction, and c is the speed of light. With our convention that energies are measured from the nominal band edge, we have $E_2 = E - E_g - E_1$, where E is the photon energy and E_g is the nominal energy gap. The right-hand side of (6a) must be summed over all pairs of bands between which

transitions are calculated. In our case we include transitions to the conduction band from both the heavy hole band and the light hole band.

The wave functions of states in the conduction and valence bands have been given in the previous section; the matrix element which connects them in optical transitions is the matrix element of the momentum operator. In evaluating that matrix element, and in the spirit of the effective-mass approximation, we assume that the envelope function is more slowly varying than the Bloch function u , so that the dominant contribution to the matrix element of the momentum operator comes from the periodic part of the Bloch functions in a single lattice cell, and the remaining integration can be carried out over all space. Thus we obtain

$$\begin{aligned} \langle \psi_c | \vec{p} | \psi_v \rangle &\sim \langle u_c | \vec{p} | u_v \rangle \\ &\times \int e^{-i(\vec{k}_c + \vec{k}_{c0} - \vec{k}_v) \cdot \vec{r}} e^{-\beta_c |\vec{r} - \vec{r}_{c0}|} e^{-\beta_v |\vec{r} - \vec{r}_{v0}|} d^3\vec{r}. \quad (7) \end{aligned}$$

Note that the matrix element of \vec{p} between Bloch states at different points in the Brillouin zone does not necessarily vanish. The familiar \vec{k} selection rule which requires that optical transitions take place with negligible wave-vector change arises only when the $e^{i\vec{k}_{c0} \cdot \vec{r}}$ factor is included with the wave function. In our calculation, localization of the envelope functions contributes Fourier components which help break the \vec{k} selection rule. The role of phonons is discussed below.

The matrix element $\langle u_c | \vec{p} | u_v \rangle$ in (7) has been estimated for transitions between the top of the valence band and the bottom of the conduction band of Si from the $\vec{k} \cdot \vec{p}$ expansion of Cardona and Pollak,¹⁹ and is found to have a value of 0.4 a.u., about 60% as large as the corresponding matrix element in the direct-gap III-V semiconductors. We note in passing that the corresponding matrix element connecting the top of the valence band and the bottom of the conduction band in Ge is found to be only about one-fourth as large as the value we find for Si.

To evaluate the matrix element (7), we need to know the spatial correlation between the positions \vec{r}_{c0} and \vec{r}_{v0} of the conduction- and valence-band states. There is expected to be some correlation, because the states far in the conduction-band tail arise from a large negative excursion of the fluctuating potential, whereas states far in the valence-band tail arise from large positive excursions. Such a pair of states is likely to be more widely separated spatially than one would find from a calculation which treats them as uncorrelated. If the spatial extent of the wave functions is small compared to the spatial scale of the potential fluctuations, so that there is negligible tunneling through potential barriers, the correlations be-

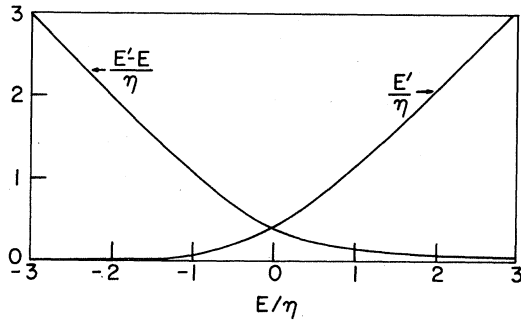


FIG. 2. Variation of E' with E and of $E' - E$ with E . The zero of energy is at the nominal band edge, and energies in the tail are negative. The unit of energy is the band-tail parameter η in the Kane function [see Eq. (48) of Ref. 13].

tween the centers of the conduction- and valence-band wave functions lead to the result that tails in the density of states do not give rise to tails in the optical-absorption spectrum.²⁰

In this work we make the assumption that there is substantial tunneling of the wave functions through the potential barriers. We do not have a good model for the correlations, and for the present we simply average the square of the matrix element (7) over all relative positions of \vec{r}_{c0} and \vec{r}_{v0} . The resulting matrix element is

$$M_{av}^2 = M_b^2 M_{env}^2, \quad (8a)$$

$$M_b^2 = \frac{1}{6} |(u_c | \vec{p} | u_v)|^2, \quad (8b)$$

$$M_{env}^2 = \frac{64}{3} \pi b [(b^4 - 5B^2b^2 + 5B^4)(3t^4 + q^4)(t^4 - q^4)^{-3} + 8b^2B^2t^2(3b^2 - 10B^2)(t^4 + q^4)(t^4 - q^4)^{-4} + 16b^4B^4(5t^8 + 10t^4q^4 + q^8)(t^4 - q^4)^{-5}], \quad (8c)$$

where $B^2 = \beta_c \beta_v$, $b = \beta_c + \beta_v$, $t^2 = b^2 + |\vec{k}_c + \vec{k}_{c0}|^2 + k_v^2$, and $q^2 = 2|\vec{k}_c + \vec{k}_{c0}|k_v$. The factor $\frac{1}{6}$ in Eq. (8b) arises because we average over all directions of polarization of the radiation and because we average over spin orientations. When k_{c0} is nonzero, as for Si, we must average the squared matrix element over all orientations of \vec{k}_c with respect to \vec{k}_{c0} , taking the conduction-band mass anisotropy into account. That average is taken numerically in our calculation.

Phonon-induced transitions are present in the optical absorption of crystalline Si, and will be present in amorphous Si as well. We take them into account by calculating the value of the squared matrix element which must be used in (6) to give the measured optical absorption of crystalline Si at 2 eV, and assuming it to be a constant independent of E_1 and E_2 . The values we find are 6×10^{-23}

$\text{g}^2 \text{cm}^5 \text{sec}^{-2}$ at 300 °K and $3 \times 10^{-23} \text{g}^2 \text{cm}^5 \text{sec}^{-2}$ at 77 °K; absorption data for crystalline Si obtained by Dash and Newman²¹ have been used.

The optical absorption of amorphous Si has been calculated as described above and has been compared with measurements on sputtered Si films deposited at room temperature and annealed at 298 and at 500 °K.²² The only adjustable parameter in the theory is the magnitude of V_{rms} , and we adjust that value to obtain good agreement with the absorption coefficient in the low-energy range. We find, however, that agreement at photon energies above 1.5 eV cannot be obtained with any value of V_{rms} , and interpret this to mean that the Fourier transform of our wave function (2) does not have enough amplitude at large values of k . To rectify the discrepancy with experiment, we have changed the band structure on which the calculation is based, since this is numerically simpler than changing the wave function. A reduction of k_{c0} from 9.5×10^7 to $6 \times 10^7 \text{cm}^{-1}$ is sufficient to give good agreement with experiment to 2 eV. We regard this change as an artifice to overcome the deficiencies in our wave function, but the possibility that it has physical significance cannot be entirely ruled out. The location of the conduction-band minimum in Si is not determined by symmetry and may well be different in amorphous than in crystalline material, in fact it has any signifi-

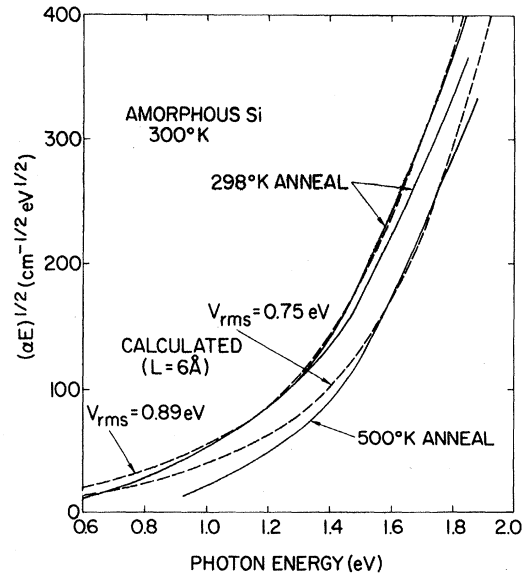


FIG. 3. Optical-absorption coefficient α (at room temperature) of amorphous Si films annealed at 298 and at 500 °K, plotted as $(\alpha E)^{1/2}$ vs photon energy E . The experimental results are from Ref. 22. The calculated results are obtained using a wave-vector separation of $6 \times 10^7 \text{cm}^{-1}$ between conduction- and valence-band edges. See Ref. 23a.

cance at all in the amorphous material.²³

Figure 3 shows a comparison of our calculated results with experiment. The values of V_{rms} which give good agreement with the optical absorption of the 298 and 500 °K annealed samples are 0.89 and 0.75 eV, respectively. The agreement for the sample annealed at room temperature is striking but fortuitous in view of the many approximations we have made.^{23a}

Figure 4 includes additional data for several amorphous Si samples as reported by Beaglehole and Zavetova.²⁴ The variation of the absorption edge from sample to sample is accounted for in our model by a variation in the magnitude of the potential fluctuations. Annealing at higher temperatures leads to smaller fluctuations in this picture.

The matrix element connecting conduction- and valence-band states is a function of the energy of both states, and is not easily graphed. We can show, however, the squared matrix element for that pair of energies which gives the greatest contribution to the absorption coefficient for each photon energy E .²⁵ Such a plot is given in Fig. 5,^{23a} where the values have been normalized by dividing them by the constant value of the squared matrix element which we used to account for the phonon-induced optical absorption. At low photon energies the plotted matrix element in Fig. 5 is small because the wave functions deep in the band tails overlap very little on the average even when spatial correlations are ignored. For $V_{rms}=0.75$ eV the matrix element rises quite sharply with increasing photon energy and depends sensitively on the value of k_{c0} . That behavior does not appear to be physically reasonable, and probably represents a defect of our model.

In Fig. 4 it is evident that our calculation overestimates the absorption at low photon energies. Even sharper absorption edges are found in other samples, particularly for Ge.²⁶ The spatial correlation of wave functions far in the tail would lead

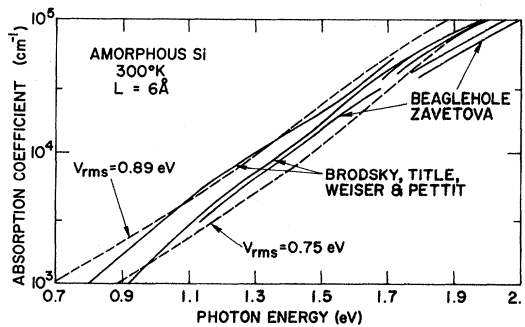


FIG. 4. Logarithm of optical-absorption coefficient vs photon energy. Data from Refs. 22 and 24 are shown, and represent different sample preparation and annealing histories. Calculated curves are the same as in Fig. 3.

to smaller values for the matrix element than those calculated in our model, and would also reduce the phonon-induced transitions below the levels we estimate. Coulomb interaction between electron and hole, also neglected here, will tend to increase the absorption coefficient near the edge. The spatial correlation of the wave functions is likely to be the dominant effect in the tail, and will reduce the absorption coefficient below the values we calculate.

V. MOBILITY EDGE

A number of authors²⁷ have discussed the existence of a mobility edge separating localized from delocalized states in a semiconductor energy-band tail. In this section we use a quantitative, albeit speculative, model to determine the position and properties of the mobility edge.

To characterize the electrical transport properties, we want to find an effective bandwidth associated with the overlap of wave functions near a given energy, and we want to find the effective spacing of the localization centers \vec{r}_{i0} of these wave functions. The scheme which follows is guided by the expectation that the bandwidth will be large and the average spacing will be small for states with energies within the band, whereas the bandwidth will be small and the spacing large for states far in the tail.

Let us first suppose that we know the bandwidth $W_i(E)$ for band i . Then we define the spacing parameter $r_{s,i}$ by the requirement that the sphere of radius r_s will, on the average, hold one state within the bandwidth W_i . Thus

$$\frac{4}{3} \pi r_{s,i}^3(E) = [\rho_i(E) W_i(E)]^{-1}. \quad (9)$$

We now assume that the bandwidth is the same function of r_s as in a regular lattice, and approximate the Brillouin zone for such a lattice by a sphere of radius $(\frac{9}{2} \pi)^{1/3} / r_s$. Then

$$W_i = (\frac{9}{2} \pi)^{2/3} \hbar^2 / 2m_i^*(E) r_{s,i}^2(E), \quad (10a)$$

$$m_i^*(E) = \kappa \hbar^2 \beta_i(E) / e^2 \alpha(x_s), \quad (10b)$$

$$x_s = \beta_i(E) r_{s,i}(E). \quad (10c)$$

The effective mass is taken to be that associated with a Bohr radius equal to β_i^{-1} , where $\beta_i(E)$ gives the localization of the wave function in (2). The effective mass (10b) contains the dielectric constant κ , and is implicitly tied to a hydrogenic model of energy levels, although Coulomb centers are not expected to be the source of the potential fluctuations. The effective mass also contains the factor α^{-1} which gives the increase in effective mass²⁸ with increasing values of x_s , the dimensionless average Wigner-Seitz radius for our problem. The variation of α with x_s is shown in Fig. 6.

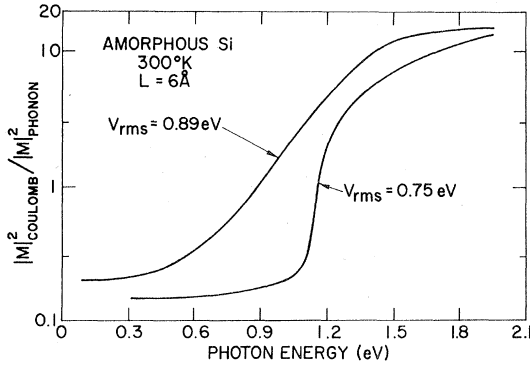


FIG. 5. Ratio of squared Coulomb matrix element calculated in this work to the squared matrix element for phonon-assisted transitions. The Coulomb matrix element is given for the transition which contributes most to the absorption coefficient at the indicated photon energy. Same parameters as for Figs. 3 and 4. See Ref. 23a.

The foregoing equations can be combined to give

$$x_s \alpha(x_s) = \frac{3}{2\pi} \left(\frac{9}{2\pi} \right)^{2/3} \frac{\kappa \beta_i^2(E)}{e^2 \rho_i(E)}. \quad (11)$$

All the quantities on the right-hand side in (11) are known from our model, so we can use the curve of $x_s \alpha(x_s)$ vs x_s in Fig. 6 to determine x_s , and can then use (10) to determine r_s and the bandwidth W for each energy. Our model loses validity at high energies, where the predicted value of r_s decreases to atomic separations and the bandwidth increases to many electron volts. Also, we find from Fig. 6 that there are no real values of x_s which satisfy Eq. (11) when $x_s \alpha(x_s) > 2.32$; thus, this model breaks down far in the tail. In this region we must replace W in Eq. (9) by another width. If that width is a constant, then the resulting value of r_s will be less strongly dependent on ρ than at higher energies, but the bandwidth deduced from r_s via Eq. (10) will vary rapidly with energy because of the rapid increase of α^{-1} with x_s when x_s exceeds 4. This variation in the bandwidth might give rise to a recombination edge, as seen in photoconductivity measurements on amorphous chalcogenide films³⁰ and in measurements of the mobility of electrons injected into amorphous Si films prepared by glow-discharge decomposition of silane.³¹

Results for the spacing r_s and bandwidth W in the energy range in which our model is applicable, as well as the values of ρ and β on which they are based, are shown in Fig. 7 for the valence and conduction bands of room-temperature-annealed amorphous Si, using the same input parameters that were used in calculating the optical absorption in Sec. IV. All the quantities have the qualitative variation with energy that we expect; the bandwidth W has a particularly strong dependence on

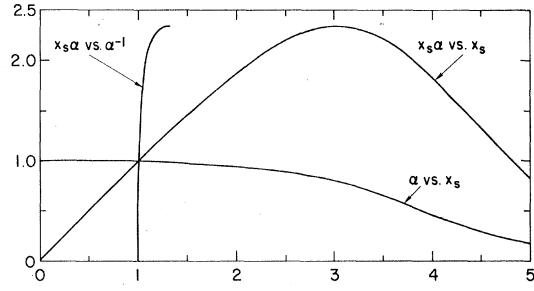


FIG. 6. The quantity α of Eq. (10b), whose reciprocal gives the increase in effective mass, is plotted vs the dimensionless Wigner-Seitz radius x_s . Also shown are the functions $x_s \alpha(x_s)$ [used in Eq. (11)] vs x_s and $x_s \alpha(x_s)$ vs α^{-1} .

energy.

We now have the information we need to find the mobility edge. The Anderson³² criterion for localization is approximately given by $\Delta \approx 9(z - 2.5)W/z$,³³ where W is the bandwidth, Δ is the spread of potentials in Anderson's model (called W in Ref. 32), and z is the number of nearest neighbors at each

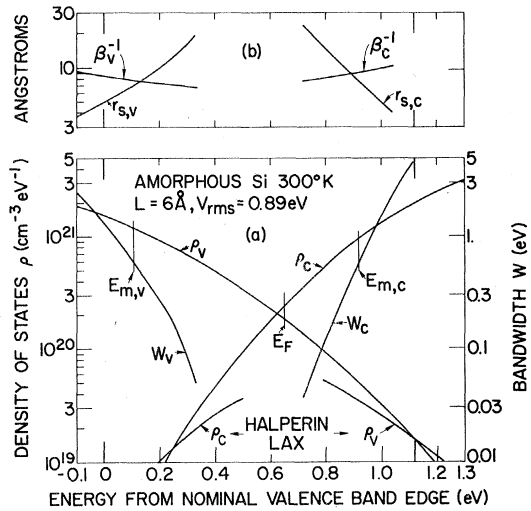


FIG. 7. Calculated results using the parameters for amorphous Si annealed at room temperature. (a) Density of states and bandwidth as functions of energy from the nominal (unperturbed) valence-band edge. The nominal conduction-band edge is at 1.12 eV. The two short curves near the bottom give the Halperin-Lax (Ref. 4) densities of states for the conduction and valence bands to their limit of validity. For the reason given in Ref. 11, the Halperin-Lax density of states for the conduction band has not been multiplied by a factor 6 for valley degeneracy. The full density-of-states curves are obtained by matching a one-parameter Kane function (Ref. 13) to the Halperin-Lax results at one energy in the tail and to the unperturbed band results at very high energy. (b) Localization distance β^{-1} and spacing parameter r_s as functions of energy.

site. Anderson assumed that the fluctuating potential had equal likelihood of lying anywhere within a band of width Δ . The root-mean-square fluctuation of Anderson's model is $\Delta/(12)^{1/2}$, which we identify with V_{rms} in our model. The coordination number z is not well defined in our case, since it applies to the random locations of the centers \vec{r}_{i0} of the wave functions.³⁴ We use $z=6$ to obtain the approximate criterion

$$W_i(E_{m,i}) \sim \frac{2}{3} V_{\text{rms}} \quad (12)$$

for the mobility edge $E_{m,i}$ which separates the localized states far in the tail of band i from the delocalized states at higher energy. The corresponding values for the amorphous Si case illustrated in Fig. 7 are shown there as vertical lines. Numerical values of some physical quantities associated with the calculation are given in Table I.

Note that the localization parameter β varies smoothly through the mobility edge, even though that edge represents a separation between localized and delocalized states. We can resolve the dilemma if we note that Eq. (2) describes the wave function of energy E only in the neighborhood of \vec{r}_{i0} . At some distance from \vec{r}_{i0} the electron will encounter another local potential minimum, near which the wave function can again be approximated by an expression like (2). The complete wave function is formed by joining these local wave-function segments together. We understand the Anderson theorem in this context to mean that the probability of the resulting wave function having appreciable amplitude far from \vec{r}_{i0} vanishes for energies below $E_{m,i}$.

The mobility above the mobility edge can be estimated from the same model. We assume that the diffusion constant for carriers at energy E is^{35,36}

$$D_i(E) = r_{s,i}^2(E) W_i(E) f_i(E) / 6h, \quad (13)$$

where h is Planck's constant and $f_i(E)$ is a dimensionless factor to take correlations between sites into account. The mobility obtained from (13) at room temperature via the Einstein relation is given in Table I for the mobility edge of each band, using $f_i=1$.

The mobility values we find are all about $5 \text{ cm}^2/\text{V sec}$, consistent with the values deduced by LeComber and Spear³¹ from mobility measurements on electrons injected into amorphous Si prepared by glow-discharge decomposition of silane. Weiser, Fischer, and Brodsky³⁰ find similar values in amorphous $2\text{As}_2\text{Te}_3 \cdot \text{As}_2\text{Se}_3$.

The mobility estimated from (13) with $f=1$ is a slowly varying function of energy, and has no structure near the mobility edge. The sharp cutoff at the edge is here contained in the factor f . The Anderson theorem³² gives $f=0$ below the mobility edge. This work provides a quantitative model to

which the Anderson theory can be applied.

In the last three lines of Table I we list three dimensionless parameters which are of interest in characterizing the mobility edge. The first is the value of x_s , the dimensionless spacing parameter, which is about 0.9 for all the cases we studied. That value is surprisingly small; the value of x_s at which a sharp drop in conductivity occurs in impure semiconductors is closer to 2.5.³⁷ The second is the ratio of the mobility-edge energy to the band-tail parameter η . Our values are smaller in magnitude than the value -0.52 deduced by Eggarter and Cohen³⁸ for a system of hard-core scatterers. Finally, we give the ratio of the parameters k and β of Eq. (2), evaluated at the mobility edge. The ratio is greater than unity, indicating that the wave function has substantial oscillatory character.

VI. CONDUCTIVITY

The results in Table I can be compared directly with the measured conductivity of amorphous Si layers.²² At room temperature the measured resistivity of layers annealed at room temperature is $9 \times 10^4 \Omega \text{ cm}$, and the calculated value is $1.4 \times 10^3 \Omega \text{ cm}$. The measured activation energy between 200 and 298 °K is 0.13 eV, while the calculated value is 0.25 eV. The calculation uses $V_{\text{rms}} = 0.89 \text{ eV}$, which gives best agreement with the optical absorption of the films annealed at room temperature. The extent of the disagreement between calculated and measured activation energies is comparable for the sample annealed at 500 °K. Thus we do not correctly describe the energy levels of these samples. Our calculated Fermi level appears to be too close to the conduction band. But its location is a sensitive function of the effective masses used in the calculation, and is subject to considerable uncertainty.

If the Fermi level is in fact lower than our model predicts, then the measured conductivity of the amorphous Si films annealed at 298 and at 500 °K might be accounted for by a group of levels closer to the conduction band, perhaps associated with the defects that give rise to the spin-resonance signal.⁹ Such levels have been proposed by Davis and Mott² and by Cohen,³ but are outside the scope of this calculation. (See note added in proof.)

The extrapolated conductivity C at infinite temperature, which enters in

$$\sigma = C e^{-\Delta E/KT}, \quad (14)$$

can also provide a test of our model. To estimate C we assume that the current is carried by carriers above the mobility edges, with concentration for band i given by $KT\rho_i(E_{m,i})$. The mobility is taken to be $\mu_i(T) = eD_i/KT = 300\mu_i(300^\circ\text{K})/T$, with D_i given by (13) with $f_i=1$. The conductivity acti-

vation energy is assumed to have a temperature coefficient β' , whose value is half of the temperature coefficient of the energy gap if the Fermi level is in the middle of the gap. Under these conditions we find³⁹

$$C_i = 300 K e \rho_i(E_{m,i}) \mu_i (300^\circ \text{K}) e^{-\beta'/K}. \quad (15)$$

If both bands contribute equally to the current, the total C is the sum of the values for the conduction and valence bands.

For room-temperature-annealed Si we deduce $C_c + C_v = 400 \Omega^{-1} \text{cm}^{-1}$. Experimental values of the order of $10^4 \Omega^{-1} \text{cm}^{-1}$ ⁴⁰ and of order $1 \Omega^{-1} \text{cm}^{-1}$ ³¹ have been reported for amorphous Si, the latter for silane-grown films. Values between 0.62³¹ and 0.85 eV⁴⁰⁻⁴² have been reported for the conductivity activation energy. Our model is not likely to lead to an activation energy for Si which is much larger than 0.6 eV, half of the energy gap extrapolated to absolute zero, even with values of V_{rms} smaller than those used here. The occurrence of larger activation energies may mean that the crystalline band structure is not a valid starting point for our model. It is possible that the conduction-band minima at L are preserved in the amorphous material, because this corresponds to the bonding directions, whereas the minima along the $\langle 100 \rangle$ directions in the Brillouin zone lose their significance. If so, our model could be applied with appropriate changes in the band gap, effective masses, and matrix elements.

VII. CONCLUSIONS

We have shown how a model which treats amorphous silicon as a strongly perturbed crystal, with a perturbing potential characterized by a large amplitude V_{rms} and a small correlation length L , can be applied to the optical and electrical properties of the material. The model includes assumptions about the nature of the local wave functions in the system, and about the optical matrix elements which connect them. It invokes the Anderson

theorem to deal with the mobility edge that separates localized from delocalized states. Good agreement with optical-absorption data for amorphous Si can be obtained by appropriate choice of V_{rms} , using a value of L suggested by the radial distribution function. The high values of absorption coefficient found at photon energies near 2 eV can be explained in this model only if the wave-vector difference between the conduction- and valence-band extrema is reduced to about two-thirds of its value in the crystal. Comparison of calculated and measured electrical quantities is less clearcut. The mobility we find above the mobility edge is in good agreement with values deduced from experiment. The experimental information on the activation energy is somewhat conflicting, but at least some values are higher than those that would be expected from our model. (See note added in proof.) The calculated value of the dimensionless spacing parameter x_s at the mobility edge is lower than expected.

Every step of our model is uncertain at least by a numerical factor of order unity. It is our hope that further work will lead to a better determination of these factors and to better agreement with experiment. The model is useful in giving a microscopic picture that can be applied both to optical and to electrical properties of amorphous semiconductors.

Note added in Proof. A recent calculation^{38a} of hopping conduction near the Fermi level^{38b} suggests that the hopping conductivity is comparable to the conductivity of carriers above the mobility edge near room temperature, and exceeds it at lower temperatures, for the samples considered here. This helps to resolve some of the discrepancies noted above.

ACKNOWLEDGMENTS

I am indebted to M. H. Brodsky, B. I. Halperin, E. O. Kane, T. Kasuya, T. N. Morgan, N. F. Mott, and K. Weiser for helpful discussions during the course of this work.

¹See, for example, the papers in J. Non-Crystalline Solids 4, (1970).

²E. A. Davis and N. F. Mott, Phil. Mag. 22, 179 (1970); see also the earlier papers in the series by these authors.

³M. H. Cohen, *Proceedings of the Tenth International Conference on the Physics of Semiconductors* (U. S. Atomic Energy Commission, Oak Ridge, 1970), p. 645; see also p. 391 of Ref. 1.

⁴B. I. Halperin and M. Lax, Phys. Rev. 148, 722 (1966).

⁵M. V. Coleman and D. J. D. Thomas, Phys. Status Solidi 24, K111 (1967); S. C. Moss and J. F. Graczyk, *Proceedings of the Tenth International Conference on the Physics of Semiconductors* (U. S. Atomic Energy Commission, Oak Ridge, 1970), p. 658.

⁶V. L. Bonch-Bruевич, Dokl. Akad. Nauk SSSR 189, 505 (1969) [Soviet Phys. Doklady 14, 1101 (1970)]; J. Non-Crystalline Solids 4, 410 (1970).

⁷F. Herman and J. P. Van Dyke, Phys. Rev. Letters 21, 1575 (1968).

⁸D. Brust, Phys. Rev. 186, 768 (1969).

⁹M. H. Brodsky and R. S. Title, Phys. Rev. Letters 23, 581 (1969); R. S. Title, M. H. Brodsky, and B. L. Crowder, *Proceedings of the Tenth International Conference on the Physics of Semiconductors* (U. S. Atomic Energy Commission, Oak Ridge, 1970), p. 794.

¹⁰For definitions of the effective masses see, for example, R. A. Smith, *Semiconductors* (Cambridge U. P., Cambridge, England, 1961), pp. 81 and 99; W. G. Spitzer and H. Y. Fan, Phys. Rev. 106, 882 (1957).

¹¹B. I. Halperin (private communication) has suggested

that heavy mass components should be weighted somewhat more strongly in the effective mass that enters in Eq. (5.9) of Ref. 4 than they are in the conductivity mass. Note that the density of states in Eq. (5.8) of Ref. 4 makes no allowance for multiple band edges. The density of states for the conduction band of Si should therefore be multiplied by 6, the valley degeneracy, to give the total density of states. We have not made that correction in this work because it is counteracted by the fact that only one level associated with a given potential minimum can be occupied; the Coulomb energy will prevent a second electron from occupying one of these levels. Since the Halperin-Lax results presumably include a factor 2 for the spin degeneracy, they may already overestimate the density of states that can be occupied by electrons, even when we do not multiply by the valley degeneracy. A proper treatment of these effects requires the abandonment of the independent one-electron picture. Some aspects of the theory including electron-electron correlations have been discussed by M. Pollak [Discussions Faraday Soc. 50 (1971)].

¹²E. O. Kane, Phys. Rev. 131, 1532 (1963).

¹³E. O. Kane, Phys. Rev. 131, 79 (1963).

¹⁴V. L. Bonch-Bruевич, Fiz. Tverd. Tela 4, 2660 (1962) [Soviet Phys. Solid State 4, 1953 (1963)]; I. V. Andreev, Zh. Eksperim. i Teor. Fiz. 48, 1437 (1965) [Soviet Phys. JETP 21, 961 (1965)]; A. B. Almazov, Fiz. Tverd. Tela 5, 1320 (1963) [Soviet Phys. Solid State 5, 962 (1963)].

¹⁵F. Stern (unpublished).

¹⁶G. Lasher and F. Stern, Phys. Rev. 133, A553 (1964).

¹⁷Preliminary reports on our model for optical absorption have been presented earlier: F. Stern, Bull. Am. Phys. Soc. 14, 396 (1969); J. Non-Crystalline Solids 4, 256 (1970). Results of the model as applied to impure GaAs are being prepared for publication (Ref. 15).

¹⁸For alternative treatments of optical absorption in amorphous semiconductors, see J. Tauc, Mater. Res. Bull. 5, 721 (1970); D. Brust, Phys. Rev. Letters 23, 1232 (1969); see also Ref. 8.

¹⁹M. Cardona and F. H. Pollak, Phys. Rev. 142, 530 (1966).

²⁰See, for example, L. V. Keldysh and G. P. Proshko, Fiz. Tverd. Tela 5, 3378 (1963) [Soviet Phys. Solid State 5, 2481 (1964)].

²¹W. C. Dash and R. Newman, Phys. Rev. 99, 1151 (1955).

²²M. H. Brodsky, R. S. Title, K. Weiser, and G. D. Pettit, Phys. Rev. B 1, 2632 (1970); M. H. Brodsky (unpublished). I am indebted to Dr. Brodsky for permission to use these results.

²³See also the discussion at the end of Sec. VI.

^{23a}Footnote added in proof. An error has been found in the numerical procedure used to average over the directions of \vec{k}_c in the matrix element (8c). The agreement between calculated and measured values of the ab-

sorption coefficient is essentially unchanged when the corrected procedure is used, provided the wave-vector separation k_{c0} between the conduction- and valence-band edges is reduced from the value $6 \times 10^7 \text{ cm}^{-1}$ used previously to $5.8 \times 10^7 \text{ cm}^{-1}$. The matrix elements are smaller at the upper end of the energy range than those shown in Fig. 5, but the qualitative features are unchanged.

²⁴D. Beaglehole and M. Zavetova, J. Non-Crystalline Solids 4, 272 (1970).

²⁵B. Kramer, K. Maschke, P. Thomas, and J. Treusch, [Phys. Rev. Letters 25, 1020 (1970)] have treated the optical absorption of amorphous Se using an empirically determined matrix element which depends on photon energy.

²⁶T. M. Donovan, W. E. Spicer, and J. M. Bennett, Phys. Rev. Letters 22, 1058 (1969); K. L. Chopra and S. K. Bahl, Phys. Rev. B 1, 2545 (1970); T. M. Donovan, E. J. Ashley, and W. E. Spicer, Phys. Letters 32A, 85 (1970).

²⁷See, for example, E. N. Economou and M. H. Cohen, Mater. Res. Bull. 5, 577 (1970), and references cited therein. See also Refs. 1-3.

²⁸F. Stern and R. M. Talley, Phys. Rev. 100, 1638 (1955), Eq. (16), and Tables I and II; N. H. March, Physica 22, 311 (1956); F. Stern, Bull. Am. Phys. Soc. 1, 214 (1956).

²⁹Equation (11) has two solutions when $x_s \alpha(x_s) < 2.32$. On physical grounds we choose the solution $0 < x_s < 3$.

³⁰K. Weiser, R. Fischer, and M. H. Brodsky, *Proceedings of the Tenth International Conference on the Physics of Semiconductors* (U. S. Atomic Energy Commission, Oak Ridge, 1970), p. 667.

³¹P. G. Le Comber and W. E. Spear, Phys. Rev. Letters 25, 509 (1970).

³²P. W. Anderson, Phys. Rev. 109, 1492 (1958).

³³See also the second footnote on p. 13 of N. F. Mott, Phil. Mag. 22, 7 (1970).

³⁴An alternative approach which does not depend on coordination number may be possible. See H. Scher and R. Zallen, J. Chem. Phys. 53, 3759 (1970).

³⁵M. H. Cohen, J. Non-Crystalline Solids 4, 391 (1970), Eq. (6.6).

³⁶J. R. Manning, Phys. Rev. 139, A126 (1965), Eq. (48).

³⁷N. F. Mott, Phil. Mag. 6, 287 (1961), Eq. (5).

³⁸T. P. Eggarter and M. H. Cohen, Phys. Rev. Letters 25, 807 (1970).

³⁹Similar expressions have been obtained by many authors; see, for example, Davis and Mott, Ref. 2. Note that our coefficient β' is negative for Si.

⁴⁰R. Grigorovici, Mater. Res. Bull. 3, 13 (1968).

⁴¹C. J. Mogab and R. G. Block (unpublished).

⁴²R. C. Chittick, J. Non-Crystalline Solids 3, 255 (1970).

⁴³F. Stern (unpublished).

⁴⁴N. F. Mott, Phil. Mag. 19, 835 (1969), Sec. 6.